NeuroImage 203 (2019) 116194

Contents lists available at ScienceDirect

NeuroImage

journal homepage: www.elsevier.com/locate/neuroimage

Short-interval intracortical inhibition in human primary motor cortex: A multi-locus transcranial magnetic stimulation study

Jaakko O. Nieminen [a,b,*,1], Lari M. Koponen [a,b,1], Niko Mäkelä [a,b], Victor Hugo Souza [a,b,c], Matti Stenroos [a], Risto J. Ilmoniemi [a,b]

[a] Department of Neuroscience and Biomedical Engineering, Aalto University School of Science, Espoo, Finland
[b] BioMag Laboratory, HUS Medical Imaging Center, University of Helsinki and Helsinki University Hospital, Helsinki, Finland
[c] Department of Physics, School of Philosophy, Science and Literature of Ribeirão Preto, University of São Paulo, Ribeirão Preto, Brazil

ARTICLE INFO

Keywords:
Multi-locus transcranial magnetic stimulation
Short-interval intracortical inhibition
Motor cortex
Motor evoked potential
Transcranial magnetic stimulation
Transducer

ABSTRACT

Short-interval intracortical inhibition (SICI) has been studied with paired-pulse transcranial magnetic stimulation (TMS) by administering two pulses at a millisecond-scale interstimulus interval (ISI) to a single cortical target. It has, however, been difficult to study the interaction of nearby cortical targets with paired-pulse TMS. To overcome this limitation, we have developed a multi-locus TMS (mTMS) device, which allows controlling the stimulus location electronically. Here, we applied mTMS to study SICI in primary motor cortex with paired pulses targeted to adjacent locations, aiming to quantify the extent of the cortical region producing SICI in the location of a test stimulus. We varied the location and timing of the conditioning stimulus with respect to a test stimulus targeted to the cortical hotspot of the abductor pollicis brevis (APB) in order to study their effects on motor evoked potentials. We further applied a two-coil protocol with the conditioning stimulus given by an oval coil only to the surroundings of the APB hotspot, to which a subsequent test stimulus was administered with a figure-of-eight coil. The strongest SICI occurred at ISIs below 1 ms and at ISIs around 2.5 ms. These ISIs increased when the conditioning stimulus receded from the APB hotspot. Our two-coil paired-pulse TMS study suggests that SICI at ISIs of 0.5 and 2.5 ms originate from different mechanisms or neuronal elements.

1. Introduction

Short-interval intracortical inhibition (SICI) has been studied extensively by administering pairs of transcranial magnetic stimulation (TMS) pulses to the primary motor cortex and by measuring motor evoked potentials (MEP) from the targeted muscle (Di Lazzaro et al., 2006). Kujirai et al. (1993) demonstrated that a weak stimulus preceding a subsequent suprathreshold test stimulus by 5 ms or less may suppress the MEP due to the latter stimulus. Epidural recordings have shown that the associated suppression of descending volleys recruited by the test stimulus occurs at the cortical level (Di Lazzaro et al., 1998; Nakamura et al., 1997). SICI is prominent at two distinct interstimulus intervals (ISI). At ISIs up to about 1 ms, it has been argued to be due to axonal refractoriness (Fisher et al., 2002; Hanajima et al., 2003; Roshan et al., 2003) or synaptic processes (Roshan et al., 2003; Vucic et al., 2009, 2011). SICI at ISIs around 2.5 ms is likely related to $GABA_A$ mechanisms (Di Lazzaro et al., 2000; Ilić et al., 2002; Ziemann et al., 1996a, 1996b). Recently, Hannah et al. (2017) observed that SICI at 1-ms ISI and at greater ISIs depend differently on the pulse duration, also indicating a different mechanism underlying SICI at different ISIs. SICI may be affected, e.g., by motor training (Raffin and Siebner, 2019) or experimental pain (Salo et al., 2019).

The suppression of MEP amplitude due to SICI depends on the intensity of the conditioning stimulus (CS) and emerges when it exceeds about 40–50% of the resting motor threshold (RMT) (Kujirai et al., 1993; Schäfer et al., 1997; Vucic et al., 2009). For relaxed muscles, inhibition at 1-ms ISI has a lower threshold than at 2.5 ms (Fisher et al., 2002). For an ISI of 3 ms and a suprathreshold test stimulus, MEP suppression is strongest when CS is around 80% RMT (Kujirai et al., 1993). At different ISIs, the observed amount of inhibition has a different dependency on the CS intensity; this may be because both SICI and short-interval intracortical facilitation (SICF) contribute to the responses (Peurala et al., 2008).

Only a few studies have addressed the question of how the location or orientation of the conditioning stimulus within the primary motor cortex (M1) affects SICI. Kujirai et al. (1993) used two figure-of-eight coils, one

* Corresponding author. Department of Neuroscience and Biomedical Engineering, Aalto University School of Science, P.O. Box 12200, FI-00076, AALTO, Finland.
E-mail address: jaakko.nieminen@aalto.fi (J.O. Nieminen).
[1] These authors contributed equally to this work.

https://doi.org/10.1016/j.neuroimage.2019.116194
Received 29 January 2019; Received in revised form 3 September 2019; Accepted 13 September 2019
Available online 13 September 2019

centered above the hand area and the other placed over the vertex, to administer conditioning (CS) and test (TS) stimuli. They reported that a CS with the coil over the vertex could suppress MEPs in the relaxed first dorsal interosseous at an intensity not itself evoking any MEPs in active hand muscles. Moreover, a CS with the coil placed over the hand area suppressed the test responses in active tibialis anterior evoked by the coil at the vertex (Kujirai et al., 1993). Ashby et al. (1999) studied SICI in an epilepsy patient using an implanted electrode array with 1-cm center-to-center electrode distances. They found no SICI when the CS was delivered through neighboring pairs of electrodes further than 1–2 cm from the test site (Ashby et al., 1999). Ziemann et al. (1996b) used two coils placed on top of each other and reported that SICI at latencies above 1 ms is independent of the CS orientation, suggesting that it is mediated by neuronal elements that are stimulated equally in all orientations.

In this study, we investigate SICI in a paired-pulse TMS setting by administering over M1 two pulses separated by only a few millimeters. We also address the mechanisms behind SICI at ISIs of 0.5 and 2.5 ms using conditioning stimuli that affect only the surroundings of the targeted spot. With these measures, we aim to quantify the extent of the region causing SICI in M1. For these purposes, we have developed a multi-locus TMS (mTMS) device, which allows us to adjust the stimulation site electronically without coil movement (Koponen et al., 2018a).

2. Materials and methods

2.1. Multi-locus transcranial magnetic stimulation

Our mTMS device allows one to shift the stimulated cortical spot electronically, i.e., without coil movement, by adjusting the relative current amplitudes (Koponen et al., 2018a) in a figure-of-eight coil and an overlapping oval coil placed in a single coil former (Fig. 1A). This transducer can translate the stimulation target in the cortex on a 30-mm-long line segment in the direction perpendicular to the peak induced electric field (E-field; Fig. 1B). The E-field profile around its maximum is similar for all target locations. The transducer is driven by custom-made electronics (Koponen et al., 2017, 2018a).

To overcome the inherently slow adjustment of the capacitor voltages, we controlled the stimulation intensity by varying the pulse durations (Peterchev et al., 2013). This allowed us to administer paired-pulse mTMS with millisecond-scale ISIs while having full control over the stimulation intensity. Specifically, in our monophasic pulse waveforms, we adjusted the duration of the initial positive phase of the stimulus so that we could obtain the desired stimulation strength, i.e., depolarization of the neuronal membrane, without changing the capacitor voltage. The duration of the final negative phase was adjusted accordingly to bring the current back to zero. For more details, see the Appendix.

2.2. Participants

Nine healthy subjects (3 females, 6 right-handed, 24–35 years old, see Table 1) participated in the study after giving their written informed consent. The study was approved by the Coordinating Ethics Committee of the Hospital District of Helsinki and Uusimaa and was carried out in accordance with the Declaration of Helsinki.

2.3. Data acquisition

The measurements were conducted over the course of several days (8 and 2 days for Subject 1 and the other subjects, respectively). Subject 8 left the study after the first day, as he experienced headache, possibly caused by the activation of scalp muscles with the oval-coil stimulation, coil pressure on the scalp, or warm (but less than 41 °C) coil bottom. Participants sat in a chair and were instructed to keep their right hand relaxed. Electromyography was recorded with the eXimia EMG device (500-Hz low-pass filtering, 3,000-Hz sampling frequency; Nexstim Plc, Helsinki, Finland) from the right abductor pollicis brevis (APB), first dorsal interosseous, and abductor digiti minimi using surface electrodes in a belly–tendon montage. Data of first dorsal interosseous and abductor digiti minimi are not considered in the present study, as the stimulation targeting was defined relative to the APB hotspot (see below).

TMS was administered with the mTMS transducer shown in Fig. 1. The position of the transducer with respect to the subject's head was monitored with the Nexstim eXimia NBS neuronavigation system. For this purpose, the participants had undergone structural T1-weighted magnetic resonance imaging; in the analysis of Experiments 1a–b and 3, the same imaging data were used for building anatomical head models of subjects. The transducer was positioned according to the global anatomy of the left M1 so that lateral target movement would keep the maximally stimulated site within M1 (see Fig. 2). The predominant E-field direction was in the posterior–anterior (PA) direction to obtain maximum MEP amplitudes, unless otherwise mentioned. The duration of the applied monophasic pulse waveform was varied to adjust the intensity (see Section 2.1), but the waveform always contained a 30-μs hold period with near-zero E-field between the parts with positive (PA direction) and negative (anterior–posterior, AP, direction) E-fields (Koponen et al., 2018b). The maximum pulse duration was 176 μs.

Table 1
Subjects. Hand preference was self-reported by the participants. RMT is given in terms of the maximum E-field intensity induced in the geometry of our TMS-coil characterizer (Nieminen et al., 2015).

Subject	Age	Gender	Handedness	RMT (V/m)
1	32	Male	Right	74
2	28	Male	Right	102
3	27	Female	Left	72
4	26	Female	Right	73
5	35	Male	Right	79
6	24	Male	Right	102
7	29	Female	Left	79
8	25	Male	Right	81
9	33	Male	Left	78

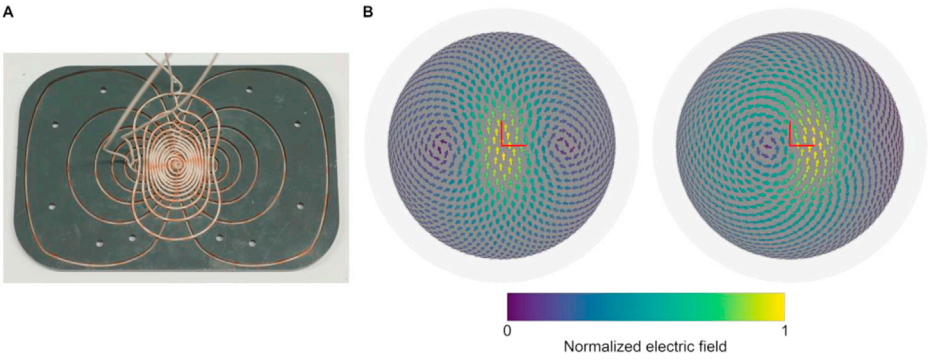

Fig. 1. mTMS transducer. (**A**) A photograph of our two-coil mTMS transducer. The figure-of-eight coil induces an E-field with its maximum below the coil center. Simultaneous activation of the overlying oval coil seamlessly moves the field maximum in the horizontal direction. The size of the coil former is 20 by 30 cm. (**B**) E-field distributions for central (left) and 15-mm-translated (right) stimulation on a spherical surface with a radius of 70 mm as measured by our TMS-coil characterizer (Nieminen et al., 2015); the bottom of the transducer was 85 mm from the origin of the spherical model. The red lines indicate the position below the transducer center.

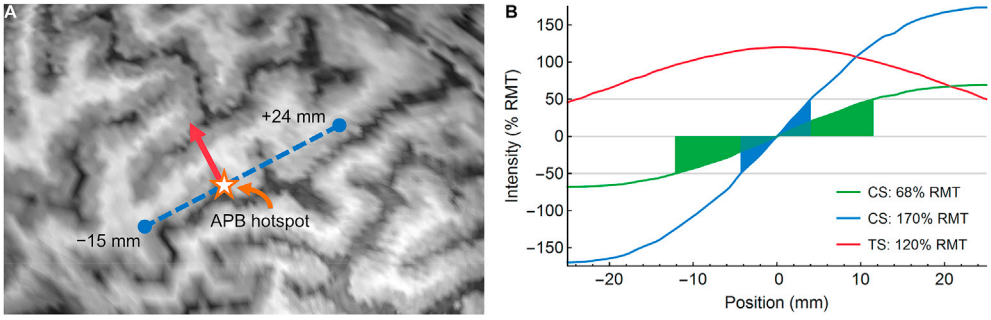

Fig. 2. Stimulation targets in paired-pulse mTMS (Experiment 1a) and E-field profiles in two-coil paired-pulse TMS (Experiment 3). (**A**) Stimulation targets overlaid on a magnetic resonance image of the primary motor cortex of Subject 1. The star indicates the location of the test-stimulus target corresponding to the APB hotspot. The red arrow gives the direction of the test stimulus. The conditioning stimuli were given along a line segment covering locations in M1 (blue dashed line). (**B**) Measured E-field profiles of the oval (CS) and figure-of-eight (TS) coil in the spherical geometry of our TMS-coil characterizer (Nieminen et al., 2015) in the direction perpendicular to the peak induced E-field of the figure-of-eight coil (along the blue dashed line in panel A). The colored shadings show the regions in which the oval-coil stimulation intensity is below 50% RMT.

Using the figure-of-eight coil alone, we first located the APB hotspot in the left M1 for each subject. Then, we determined the RMT of APB as the lowest stimulation intensity eliciting MEPs greater than or equal to 50 μV in peak-to-peak amplitude in at least 10 out of 20 consecutive trials (Rothwell et al., 1999) with a randomized ISI of 4–6 s (2–3 s for Subject 1). In this part, all pulses had a 60-μs initial phase, and the intensity was adjusted by varying the capacitor voltage. With the transducer above the APB hotspot, we mapped the motor responses elicited by single-pulse TMS on targets lateral or medial to the hotspot by electronically translating the E-field pattern to different targets. This mapping, conducted at 110% RMT (all pulses having 60-μs initial phases), covered targets located within 15 mm from the hotspot in both lateral and medial directions, in 1-mm steps. Each location was stimulated four times (three times for Subject 1), the stimulation order was randomized, and the ISI was 4–6 s.

In those paired-pulse experiments in which the transducer was above the APB hotspot (see below), the capacitor voltage of the figure-of-eight coil was set so that a pulse with a 60-μs initial phase would correspond to 100%-RMT stimulation of the APB hotspot.

2.3.1. *Experiment 1a: paired-pulse mTMS*

With Subject 1, we studied how a conditioning stimulus to the vicinity of the APB hotspot affects MEPs. We placed the transducer above the APB hotspot and applied a paired-pulse mTMS protocol with test stimuli to the APB hotspot at 120% RMT. These were preceded by a conditioning stimulus at 80% RMT, administered either at the APB hotspot or to its lateral or medial sides covering the range from −15 to 15 mm in 3-mm steps (negative and positive values refer to lateral and medial displacements, respectively; see Fig. 2A). The CS–TS interval varied from 0.5 to 10 ms (20 ISIs). Each pulse pair was administered eight times on two sessions in separate days (i.e., 16 times in total), to account for MEP variability. In both sessions, we also applied 64 test stimuli without a preceding conditioning stimulus to obtain a reliable baseline, to allow the effects of the conditioning stimuli to be determined. In addition, for each target, we administered the conditioning stimulus alone (i.e., without the test stimulus) 16 times on both days. In both sessions, the stimuli were shuffled and divided into 16 pulse sequences, with 125 stimuli each. The inter-train interval (ITI) was 4–6 s. Consecutive pulse sequences were separated by a break of a couple of minutes.

To extend the studied region to cover also medial sites with longer distances to the APB hotspot (16, 18, 20, and 24 mm), we applied a protocol in which the transducer was placed at the midpoint between the APB hotspot (test-stimulus target) and the site of the conditioning stimulus; each transducer location was used to stimulate only one CS target. The transducer was placed at the four positions in a randomized order and each position was visited four times (in total 16 pulse sequences). Each pulse sequence contained four repetitions of each ISI, 12 test stimuli alone, and four repetitions of the conditioning stimulus alone, all in a randomized order. Also in this part, ISI ranged from 0.5 to 10 ms (20 ISIs), ITI was 4–6 s, and brief breaks separated consecutive pulse sequences. The intensities of the conditioning and test stimuli were 80 and 120% RMT, respectively. Table 2 summarizes the key parameters of the experiments.

2.3.2. *Experiment 1b: paired-pulse single-site TMS on Subject 1*

The TMS-induced E-field affects a relatively broad cortical region

Table 2
Summary of experiments 1–3.

	Experiment 1a	Experiment 1b	Experiment 2	Experiment 3
Number of subjects	1	1	9 (8)	9 (8)
Conditioning-stimulus intensity	80% RMT	50–75% RMT in 5% steps	24–80% RMT in 0.5% steps (both E-field polarities)	48–170% RMT (13 intensities, both E-field polarities)
Test-stimulus intensity	120% RMT	120% RMT	120% RMT	120% RMT
Conditioning-stimulus target	−15 … 15 mm (in 3-mm steps); 16, 18, 20, or 24 mm from the APB hotspot	APB hotspot	APB hotspot	Surroundings of the APB hotspot
Test-stimulus target	APB hotspot	APB hotspot	APB hotspot	APB hotspot
Interstimulus interval	0.5–10 ms (20 ISIs)[a]	0.5–10 ms (20 ISIs)[a]	0.5 and 2.5 ms	0.5 and 2.5 ms
Inter-train interval	4–6 s	4–6 s	4–6 s	4–6 s
Number of repetitions of each paired-pulse stimulus	16	16	1	16
Number of test stimuli for reference	64 (48 for CS targets at 16, 18, 20, and 24 mm)	48	45	54

[a] The exact ISIs are provided by the small dots in Fig. 3.

even with a focal TMS coil (Nieminen et al., 2015). Consequently, in Experiment 1a, the conditioning stimulus caused a significant E-field at the hotspot even when its peak E-field targeted an adjacent site. To understand the effect of this stray E-field, we performed with Subject 1 a paired-pulse TMS experiment, in which both the conditioning and the test stimuli were administered to the APB hotspot. We varied the intensity of the conditioning stimulus from 50 to 75% RMT in 5% steps to mimic the effect of the non-zero E-field at the hotspot in Experiment 1a, in which the conditioning stimulus targeted an adjacent site. The intensity of the test stimulus (120% RMT), ISI (0.5–10 ms, 20 values), and ITI (4–6 s) matched those of Experiment 1a for direct comparison. These stimuli were divided into 16 pulse sequences, each containing one repetition of each pulse pair, three single pulses at 120% RMT, and one single pulse at each test-stimulus intensity, all in a randomized order.

2.3.3. Experiment 2: paired pulse single-site TMS on all subjects

Experiments 1a and 1b revealed that the CS intensity at the APB hotspot largely explains how a conditioning stimulus targeting the surroundings of the hotspot affect MEPs measured from APB (see Section 3.1). Therefore, Experiments 2 and 3 were conducted on all subject with the purpose of separating the effect of direct hotpot stimulation from the effect of stimulating its surroundings.

To find the threshold intensity above which a conditioning stimulus at the hotspot inhibits MEPs for each subject, we varied the intensity of the conditioning stimulus while keeping the test stimulus at 120% RMT. In this experiment, we used ISIs of 0.5 and 2.5 ms and varied the intensity of the conditioning stimulus from 24% to 80% RMT in 0.5% steps; at each ISI and intensity, we administered one stimulus. Sampling just one stimulus per intensity was selected because the average MEP amplitude can be assumed to be a smooth function of the CS intensity (Ilić et al., 2002), and consequently the typical MEP amplitude at given CS intensity can be obtained with a moving median filter over the different CS intensities. The single-pulse-per-intensity sampling also provides higher resolution on the CS threshold intensity than sampling multiple pulses per intensity for a fixed total number of stimuli. These sessions included also a similar set of stimuli in which the polarity of the conditioning stimulus was reversed to account for the opposite E-field direction on the medial and lateral sides of the APB hotspot (Fig. 2B). For reference, we had 45 single-pulse stimuli at 120% RMT. The stimulation order was randomized and the stimuli were divided into nine pulse sequences. ITI was 4–6 s.

2.3.4. Experiment 3: two-coil paired-pulse TMS

To learn how the stimulation of the surroundings of the APB hotspot contribute to the inhibition at ISIs of 0.5 and 2.5 ms, we conducted a paired-pulse experiment in which the conditioning stimulus was given by the oval coil and the test stimulus by the figure-of-eight coil (Fig. 2B; all participants included). Here, the test stimulus targeted the APB hotspot, while the conditioning stimulus affected its surroundings (the oval coil induces zero E-field at a point below its center; see Fig. 2B). The test-stimulus intensity was 120% RMT. The CS intensity was defined relative to the individual TS intensity at motor threshold based on the peak CS E-field at about 25 mm from the APB hotspot (Fig. 2B); 13 different intensities from 48% to 170% RMT were determined. The conditioning stimuli were applied with both E-field polarities, there being 16 repetitions of each pulse pair. In addition, we administered 54 single pulses at 120% RMT with the figure-of-eight coil and 10 single pulses at both E-field polarities at the maximum intensity with the oval coil. Again, the order of the pulses was randomized, and the stimuli were divided into nine pulse sequences (note that we had a set of nine pulse sequences for both 0.5-and 2.5-ms ISIs, i.e., a total of 18 pulse sequences). In this experiment, the duration of the first phase of all pulses was fixed to 81.2 μs, corresponding to 120% stimulation strength relative to that of pulses with a 60-μs first phase. The applied CS and TS intensities were realized by varying the capacitor voltages.

Because stimulation with the oval coil produced MEPs in some subjects, we conducted an additional session in which we administered single-pulse TMS with the oval coil at the intensities used in the paired-pulse sessions (intensities of the side maximums between 48% and 170% RMT). This session contained 86 pulses all at different intensities, using both E-field polarities in a random order. ISI was 4–6 s. In this part, the duration of the first phase of all pulses was fixed to 81.2 μs and the intensity was adjusted by varying the capacitor voltage. This measurement was not conducted with Subjects 1, 2, and 4.

2.4. Data analysis

Data were analyzed with Matlab R2016a or newer (The MathWorks, Inc., Natick, MA, USA) and Mathematica 11 or newer (Wolfram Research, Inc., Champaign, IL, USA). We rejected trials containing muscle preactivation, artefacts, or noise exceeding ±15 μV in amplitude in the 200-ms time window preceding TMS (for Subject 6, a threshold of ±20 μV was used for the data collected on the first day). Consequently, 2% of the trials were rejected. We determined the MEP peak-to-peak amplitude and MEP onset latency with respect to the test stimulus in the accepted trials. The MEP onset latency for each trial was obtained by visual inspection. Relative MEP amplitudes and differences in latency were obtained by comparing the medians of the corresponding paired-pulse responses to those due to single-pulse TMS in the same session. The median was preferred over the mean to reduce the effect of outliers. The latency analysis considered only those trials in which an MEP was visible; thus, for pulse pairs with the strongest inhibition, only a low number of trials was included in the analysis. For each subject, we computed the center of gravity of the electronically mapped motor responses (Wassermann et al., 1992) and determined also the locations of the maximums of these maps (supplementary material).

To estimate the extent of the cortex affected by TMS, we computed the TMS-induced E-fields using individual four-compartment head models that contain realistic scalp, skull, and cerebrospinal fluid compartments and a homogeneous isotropic brain compartment. The E-field was computed using the reciprocal surface integral approach presented in detail in (Stenroos and Koponen, 2019). Anatomical head models were built from T1-weighted magnetic resonance images segmented and meshed using SimNIBS (Windhoff et al., 2013), iso2mesh (Fang and Boas, 2009), and FreeSurfer (Fischl, 2012) software toolboxes, and the TMS coils were modeled using magnetic dipole distributions (1,656 dipoles for the figure-of-eight coil, 333 dipoles for the oval coil). The E-field was computed directly in the motor cortex on a surface mesh that had the vertex spacing of approximately 1 mm.

2.4.1. Experiments 1a and 1b: paired-pulse mTMS and paired-pulse single-site TMS on Subject 1

We used cluster-based permutation statistics (Maris and Oostenveld, 2007) to identify statistically significant differences between paired-pulse mTMS/TMS and single-pulse TMS in Experiments 1a and 1b. We applied the Mann–Whitney *U* test to obtain the *U*-statistics for the difference between the paired-pulse mTMS/TMS and single-pulse TMS data at each CS-target/intensity–ISI pair; from these statistics, we subtracted the expected statistics given no difference between the datasets. After discarding the values corresponding to data with *p*-values above 0.001 (for the null hypothesis of no difference), we computed cluster statistics by summing up the *U*-statistics of the neighboring data points (neighbors in the ISI or CS-target/intensity dimensions, the discarded points defined the cluster borders). This gave us ISIs and CS-targets/intensities belonging to several candidate clusters. We assessed the statistical significance of each of these clusters by pooling the paired-pulse and single-pulse data, by drawing 100,000 random permutations with the original sample sizes, and by computing the maximum cluster statistics for each of these permutations. Finally, we obtained a two-tailed *p*-value for each candidate cluster by comparing the original cluster statistics to the distribution of the maximum statistics in the randomized data. The clusters were considered significant at

$p < 0.001$ after a Bonferroni correction of eight (four tests for these data of Subject 1 and four tests for MEP latencies, see Section 2.4.2).

We assessed the similarity of the MEPs obtained in Experiments 1a and 1b by computing the (standardized) cross-correlation between the respective datasets. First, we linearly interpolated the data in the CS-target dimension to a grid with 0.1-mm spacings (in Experiment 1a, the original data locations in this dimension corresponded to the locations of the E-field maximums in the individual head model; the CS intensities used in Experiment 1b were converted to CS targets by considering the targets at which an 80%-RMT conditioning stimulus would cause the given intensity at the APB hotspot according to individual E-field modeling). We computed the cross-correlations for both the MEP-amplitude and MEP-latency data shifted in 0.1-mm steps in the CS-target dimension.

2.4.2. Experiment 2: paired-pulse single-site TMS on all subjects

We quantified the CS intensities at which the MEP amplitudes in Experiment 2 started to drop for each ISI and CS polarity. This was done by computing the third quartile of the relative MEP amplitudes over running windows of 80 consecutive samples of the data across subjects (approximately 10 samples per subject, or a 5%-RMT window) and detecting the intensity at which the quartile first dropped below 1.

To test the null hypothesis that the MEP latencies associated with low and high CS intensities in Experiment 2 were identical, we conducted a post-hoc analysis based on permutation statistics. We split the median difference in MEP latency (differences between paired- and single-pulse MEP latencies) to two equally large groups (split at about 50%-RMT intensity); one of them contained the data associated with low and the other one the data associated with high CS intensities. We calculated the median difference in latency over CS intensities and subjects for both groups and the difference of the group medians. Then, we pooled the data, drew 1,000,000 random permutations with equal group sizes, and computed the difference in the medians for each permutation. Finally, to obtain a two-tailed *p*-value, we compared the median difference in the original dataset to the distribution of differences in the permutated datasets. This analysis was conducted separately for the ISIs of 0.5 and 2.5 ms and both CS polarities. The *p*-values were Bonferroni-corrected by a factor of eight (four of these tests and four tests with the data of Subject 1, see Section 2.4.1).

2.4.3. Experiment 3: two-coil paired-pulse mTMS

In Experiment 3, we analyzed the MEP amplitudes as a function of the width of the cortical region where the CS intensity was below 50% RMT according to individual E-field modeling. In this experiment, the conditioning stimuli were administered with both E-field polarities. To quantify how similarly these two CS types affected the MEP amplitudes, we calculated the Pearson correlation coefficient between the related group-level datasets.

3. Results

3.1. Experiments 1a and 1b: paired-pulse mTMS and paired-pulse single-site TMS on subject 1

Fig. 3 summarizes the APB responses to paired-pulse mTMS. When the conditioning stimulus was administered to the APB hotspot, the responses were in line with earlier findings showing strongest inhibition at submillisecond (<1 ms) ISIs and at ISIs around 2.5 ms (Fisher et al., 2002; Roshan et al., 2003; Vucic et al., 2006) and facilitation at ISIs longer than 6 ms (Kujirai et al., 1993). The two dominant inhibitory ISIs extended as U-shaped bands to the lateral and medial sides of the hotspot (Fig. 3A). Facilitation appeared strongest when the conditioning stimulus was administered to the immediate vicinity of the hotspot and reduced with increasing distance from it. The conditioning stimulus at the APB hotspot showed the largest reduction in MEP latency for ISIs around 5 ms (Fig. 3B). This reduction on latency diminished for shorter and longer ISIs and as a function of distance from the hotspot. The effect of the conditioning stimulus on MEP amplitude and latency seemed to disappear when the pulse was given further than 20 mm from the hotspot. The asymmetry present in the data with respect to the APB hotspot (Fig. 3, left panels) is likely due to the cortical anatomy or the identified hotspot, which was 2.4 mm on the lateral side of the center of gravity of the mapped motor responses (Supplementary Fig. S1). Comparing the paired-pulse mTMS MEP amplitudes (Fig. 3A, left panel) to those evoked by paired-pulse TMS to the APB hotspot (Fig. 3A, right panel) suggests that the mTMS results could be explained by the intensity of the conditioning stimulus at the hotspot (or within a few millimeters from it), as the two plots appear highly similar. A similar phenomenon is visible also in the MEP latency (Fig. 3B, left and right panels). For the amplitude and latency data, the maximal cross-correlations of 0.94 and 0.77 between the datasets of Experiment 1a and 1b were obtained with shifts of 1.1 and 2.4 mm, respectively. These shifts were in line with the center of gravity of the mapped single-pulse motor responses (2.4 mm for Subject 1).

3.2. Experiment 2: paired-pulse single-site TMS on all subjects

The recorded MEP amplitudes for the ISIs of 0.5 and 2.5 ms as a function of the CS intensity in Experiment 2 are shown in Fig. 4. For the PA-directed conditioning stimulus, at 0.5-ms ISI, there was a transition from baseline MEP amplitudes to nearly complete inhibition between 40 and 70% RMT. The third quartiles of the relative MEP amplitudes fell below 1 at 45%-RMT and 52%-RMT intensity for PA- and AP-directed conditioning stimuli, respectively. When the polarity of the conditioning stimulus was reversed, the inhibition appeared weaker. For an ISI of 2.5 ms, the transition from no to complete MEP reduction seemed to start at intensities above 50% for both stimulation polarities. In this case, the third quartiles of the relative MEP amplitudes fell below 1 at 56%-RMT and 62%-RMT intensity for PA- and AP-directed conditioning stimuli, respectively. There was, however, considerable variation between subjects. Supplementary Fig. S2 illustrates how the MEP onset latency changed as a function of the CS intensity. Post-hoc analysis revealed that at the ISI of 0.5 ms, the MEP latency was about 0.4 ms longer at stronger CS intensities for both PA- and AP-directed stimulation ($p = 0.0006$ for PA-directed conditioning stimulus, and $p = 0.003$ for AP-directed conditioning stimulus; two-tailed Bonferroni-corrected *p*-values). At an ISI of 2.5 ms, we observed no statistically significant effect of the CS intensity on the MEP latency ($p = 1.0$ for PA-directed conditioning stimulus; $p = 0.59$ for AP-directed conditioning stimulus; two-tailed Bonferroni-corrected *p*-values).

3.3. Experiment 3: two-coil paired-pulse mTMS

Fig. 5 presents the MEP amplitudes obtained when the conditioning stimulus administered by the oval coil stimulated only the surroundings of the APB hotspot (for MEP latencies, see Supplementary Fig. S3). The data are visualized as a function of the width of the region where the CS intensity was below 50% RMT. According to Fig. 4, this 50%-RMT intensity roughly defines a threshold above which a conditioning stimulus inhibits MEPs. The behavior at ISIs of 0.5 and 2.5 ms was different (Fig. 5). At 0.5-ms ISI, there was no visible inhibition for most of the subjects. Instead, the MEP amplitudes were facilitated with increasing oval-coil stimulation intensities. In contrast, at an ISI of 2.5 ms, a sufficiently strong conditioning stimulus reduced the MEP amplitudes. For both ISIs, when the CS intensity was increased such that the width of the region of weak CS intensity (below 50% RMT) was reduced below about 15 mm, the responses started to deviate from those evoked at lower CS intensities. There were, however, some differences between subjects: Subjects 3 and 7 showed no inhibition at ISI = 2.5 ms, the responses of Subject 4 were inhibited at ISI = 0.5 ms, and Subject 5 behaved very differently from all the others. The positive and negative oval-coil currents resulted in similar MEP amplitudes, the correlation of the median MEP amplitudes associated with the two oval-coil current directions

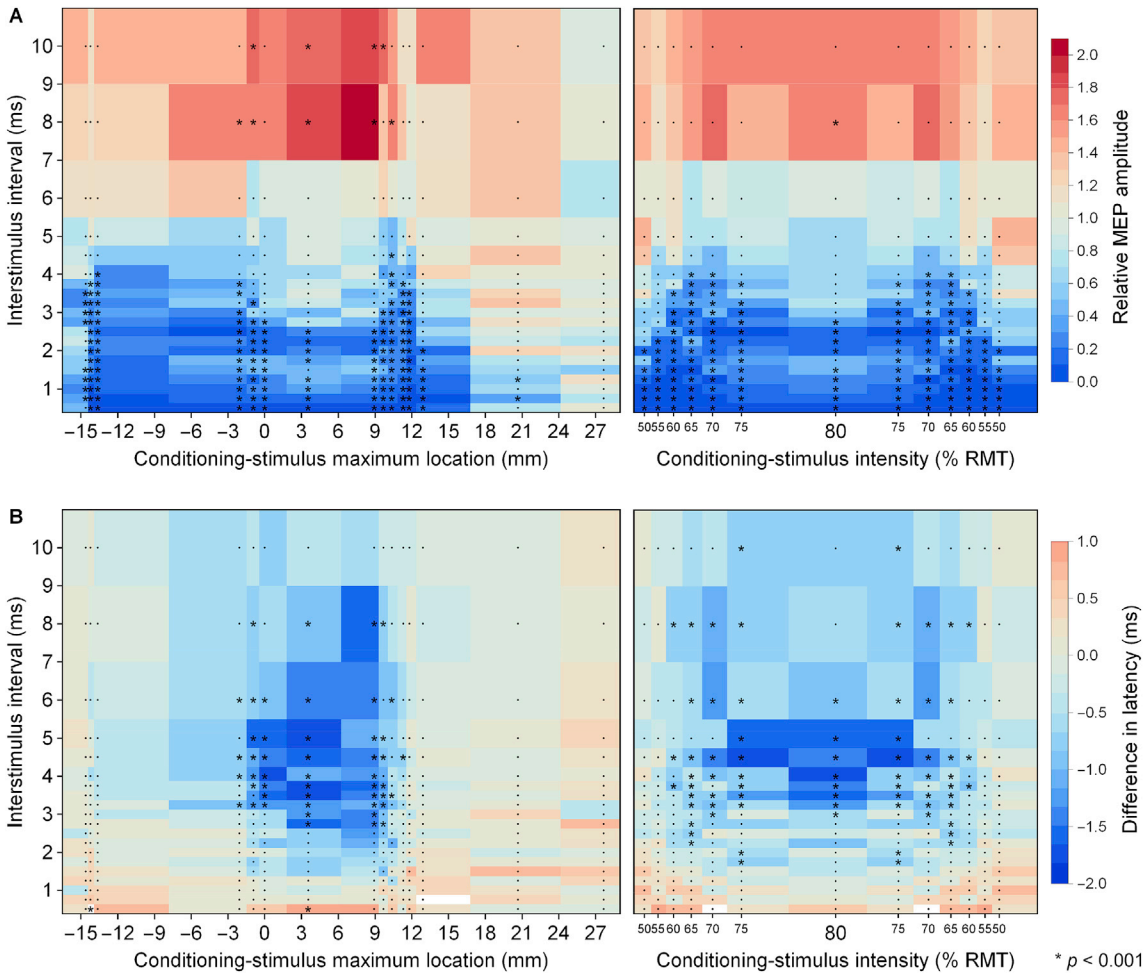

Fig. 3. Paired-pulse mTMS and paired-pulse single-site TMS on Subject 1. (**A**) Median MEP amplitudes in the paired-pulse mTMS (left) and paired-pulse single-site TMS (right) experiments. (**B**) Median differences in MEP latencies due to paired-pulse mTMS (left) and single-site TMS (right). In the left panels of (**A**) and (**B**), the horizontal axis indicates the location of the maximum of the induced E-field of the conditioning stimulus according to individual E-field modeling (two CS targets had their E-field maximum at +11.5 mm; the corresponding data are displayed at +11.25 and 11.75 mm, respectively). In (**A**) and (**B**), the asterisks indicate statistically significant differences between the paired-pulse mTMS/TMS and single-pulse TMS (two-tailed $p < 0.001$, corrected for multiple comparisons). The horizontal axes of the left and right panels are made visually comparable by spacing the CS intensities according to the CS target locations at which an 80%-RMT conditioning stimulus would cause the given CS intensity at the APB hotspot (given the individual head model); thus, 80% and 50% RMT correspond to 0 and −15.7 or +13.4 mm, respectively.

being 0.87. As shown in Supplementary Fig. S4, in all but Subjects 1 and 2, single-pulse oval-coil stimulation at the maximum intensity produced clear MEPs with both E-field polarities.

4. Discussion

In Experiment 3 (two-coil paired-pulse mTMS), we found that at ISI = 0.5 ms, motor responses were not affected when the width of the weakly stimulated region was greater than about 15 mm. In this case, the group-level results revealed no inhibition in MEPs. In contrast, we observed facilitation of the MEPs with the strongest CS intensities. This is likely because the conditioning stimuli activated surrounding facilitatory neuronal structures. This provides evidence that inhibition and facilitation are due to different cortical structures, adding to, e.g., the findings of Ziemann et al. (1996b) who showed that the inhibitory effect is independent of the direction of the induced E-field whereas the facilitation is maximized with a PA-oriented E-field. Previously, SICI at these short ISIs has been attributed to axonal refractoriness or synaptic mechanisms (Fisher et al., 2002; Hanajima et al., 2003; Roshan et al., 2003; Vucic et al., 2009, 2011). Our findings suggest that SICI at ISI = 0.5 ms is mediated by cortical structures (including those responsible for the refractoriness of the neurons) located within 8 mm from the APB hotspot, despite there being millimeter-range uncertainty in the locations of the underlying APB hotspots (see Supplementary Fig. S1). In contrast, at ISI = 2.5 ms, there is a slight reduction in the overall MEP amplitudes even when the width of the weakly stimulated region is larger. Inhibition appears at least when the width of this region is reduced below 15 mm, showing that at this ISI neuronal structures approximately 8 mm away from the APB hotspot contribute to SICI. With increasing CS intensity, the inhibition at ISI = 2.5 ms seems to turn into facilitation (Fig. 5B), likely because facilitatory neuronal structures become activated and their effect exceeds that of the inhibitory structures. This may be seen as a form of competition between SICI and SICF mechanisms (Peurala et al., 2008). Asanuma and Okuda (1962) found that in cats a small facilitatory area of pyramidal-tract neurons is surrounded by a larger inhibitory area. They also concluded that the inhibitory effect became the stronger the closer a stimulus was given to this excitatory area (Asanuma and Okuda, 1962). The behavior of the median MEP amplitudes shown in Fig. 5B is in line with their observations.

It is noteworthy that the CS polarity in Experiment 3 (two-coil paired-pulse mTMS) had minimal impact on the resulting MEPs. This implies either that the cortical structures affected by the conditioning stimuli

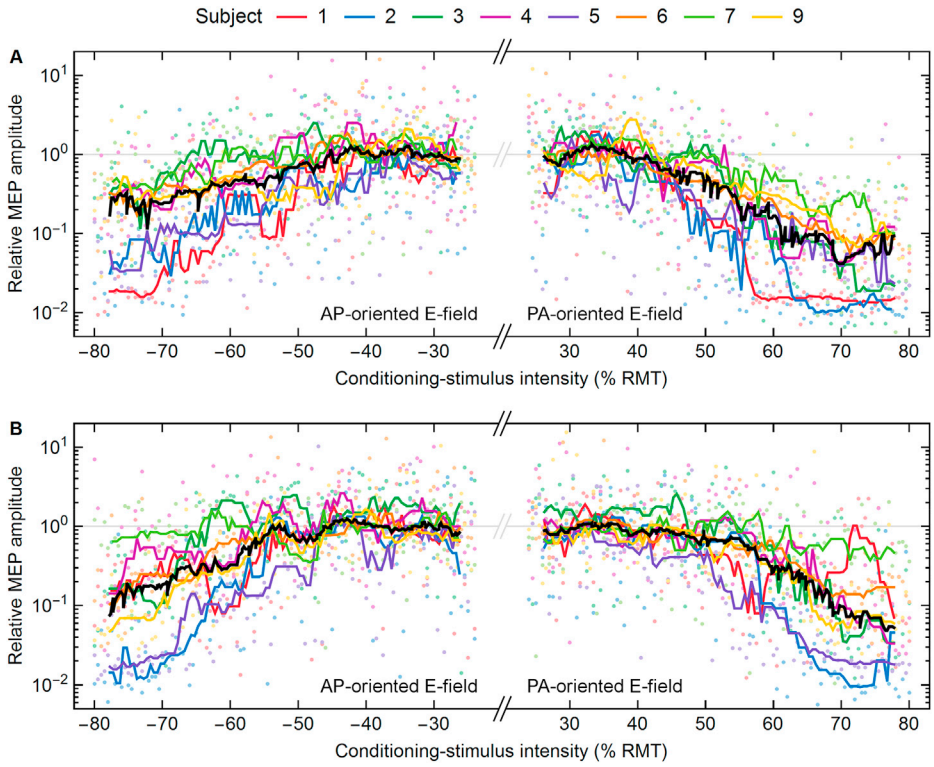

Fig. 4. MEP amplitude as a function of CS intensity. (**A**) ISI = 0.5 ms, (**B**) ISI = 2.5 ms. The colored lines display the median of 10 consecutive data points (colored dots) for each subject. The thick black lines show the median across all subjects. The data are normalized to the median MEP amplitude due to single 120%-RMT pulses. Negative CS intensities indicate AP-directed stimulation. Note the logarithmic MEP-amplitude scale.

were similar on the lateral and medial sides of the APB hotspots or that PA- and AP-oriented pulses affected these structures equally. On the other hand, in the conventional paired-pulse TMS study, PA-oriented conditioning stimuli seemed to be slightly more effective in inducing SICI than AP-oriented stimuli both at 0.5 and 2.5-ms ISI (Fig. 4). Assuming that also the structures surrounding the APB hotspot (i.e., structures stimulated with the oval coil) exhibit a similar dependency on the stimulation orientation, we may conclude that the lateral and medial sides of the APB hotspot contain cortical structures that similarly affect MEP amplitudes.

We evaluated systematically how the location of the conditioning stimulus and the ISI affect MEPs evoked by a test stimulus (Experiment 1a). We found that SICI due to a translated conditioning stimulus is similar to SICI due to a non-translated conditioning stimulus with matched E-field intensities at the targeted hotspot. The ISI exhibiting the strongest SICI seemed to increase with decreasing CS intensity at the APB hotspot being 2.0–2.5 ms at 80% MSO and about 3 ms at 60% MSO (Fig. 3A). In line with our findings on SICI, Ziemann et al. (1996b) observed that SICF in a paired-pulse TMS setting was reduced when the conditioning stimulus receded from the location of the test stimulus; their findings might also be due to the reduction of the E-field intensity of the conditioning stimulus at the motor hotspot. Thus, studies of SICI and SICF with adjacent stimuli seem to benefit from taking into account the spread of the E-field, similar to single-pulse TMS motor mappings (Bohning et al., 2001; Pitkänen et al., 2017; Thickbroom et al., 1998; Thielscher and Kammer, 2002). The focality, and thus the spread, of the E-field induced by the transducer used in this study is similar to that of commercial TMS coils (Koponen et al., 2018a; Nieminen et al., 2015). The conclusions from Experiments 1a and 1b are based on a single subject. However, given the straightforward experimental design, the simplicity of the analysis comparing the results of these two experiments, and the striking similarity of the results, we consider the conclusions well justified.

In this study, the original stimulation targets referred to the induced E-field maxima measured in a spherical head model. The locations of the peak E-field in the individual head geometry slightly differ from these values. In Fig. 3 (left panels), the clustering of the locations of the E-field maxima for the conditioning stimulus occurs because sometimes a slight change in the CS target makes the E-field maximum jump across a sulcus. Despite such nonlinear behavior of location of the E-field maximum, the E-field intensity at any location exhibits smooth behavior with respect to changes in the CS target (Fig. 3, right panels). The estimated width of the region stimulated with a weak CS intensity is based on the behavior of the modeled E-field in realistic individual geometry. Differences between the individual cortical anatomies (e.g., curvature of M1) may also explain some of the variation seen in the results. In the present study, we aimed to induce an E-field directed perpendicular to the global anatomy of the left M1; this may have resulted in suboptimal stimulation of the locations that are differently aligned (Dubbioso et al., 2017; Raffin et al., 2015). It is worth noting that in Experiment 3 (two-coil paired-pulse mTMS) responses of some participants differed from the group-level results, the reason for this remaining unknown. Thus, in addition to the group-level results, it is worth exploring the individual results. For example, in Subject 5, weak oval-coil stimulation produced no MEPs (Supplementary Fig. S4) but largely suppressed the MEP responses due to the 120%-RMT test pulses (Fig. 5). In the same subject, strong oval-coil conditioning stimuli strongly reduced the MEP onset latency unlike in the other subjects (Supplementary Fig. S3). Similarly, in this subject, MEP latencies due to single-pulse oval-coil stimulation were reduced compared to figure-of-eight-coil stimulation (Supplementary Fig. S4). This suggests that, in this subject, the oval coil activated neuronal structures that were closer to the motor output circuits than those activated with the figure-of-eight coil. In this subject, single-pulse figure-of-eight-coil stimulation at 120% RMT produced MEPs comparable to those of the other subjects. Note that due to the withdrawal of Subject 8, only eight subjects completed Experiment 3 with the 0.5-ms ISI.

Our data on the SICI as a function of the CS intensity is in line with earlier findings. We observed that inhibition at ISI = 0.5 ms emerged at

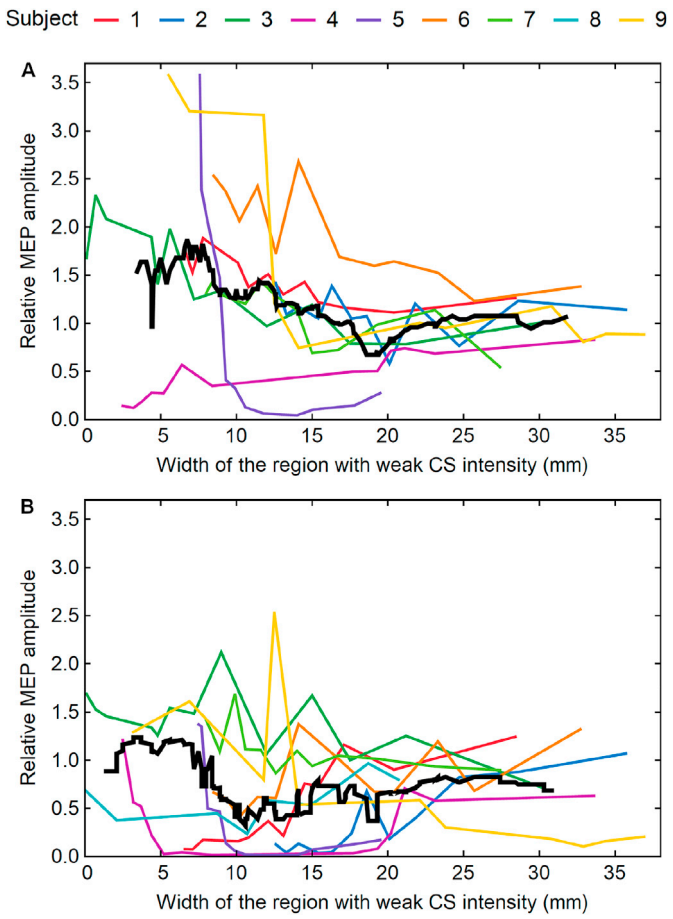

Fig. 5. Two-coil paired-pulse TMS. MEP amplitude as a function of the size of the weakly stimulated region (CS intensity <50% RMT) with an ISI of (**A**) 0.5 and (**B**) 2.5 ms. The data are displayed relative to the median MEP amplitude due to single 120%-RMT pulses. The colored lines show the median responses of individual subjects. The solid black lines display the median over all subjects.

lower CS intensities than at ISI = 2.5 ms, while also agreeing with, e.g., Kujirai et al. (1993) (ISI = 3 ms), Schäfer et al. (1997) (ISI = 1 ms), and Vaalto et al. (2011) (ISI = 2 ms) who also observed that inhibition emerged when the CS intensity reached about 50% RMT. The 0.5- and 2.5-ms ISIs for Experiments 2 and 3 were selected based on the observed strong SICI in Experiment 1 at 80%-RMT CS intensity and on the literature (e.g., Fisher et al., 2002; Roshan et al., 2003; Vucic et al., 2009). However, these ISIs may not exactly match the ones representing the strongest SICI for each subject at that CS intensity. On the other hand, based on Peurala et al. (2008), an ISI of 2.1 ms could have been advantageous to minimize the effect of SICF on the results. However, similar to the ISI corresponding to the strongest SICI (Fig. 3A, right panel), the optimal ISI to minimize the contribution of SICF may also depend on the CS intensity. Thus, a more elaborate experimental paradigm would have been needed to ensure maximal sensitivity to SICI and minimal impact of SICF.

Depending on the point of view, the inclusion of both right- and left-handed participants may be considered either as a strength or a limitation of the study. As only three left-handed participants were studied, it is hard to conclude whether some of the individual differences are due to the handedness. In Experiment 3 with the 2.5-ms ISI, however, only the three left-handed subjects (Subjects 3, 7, and 9) exhibited MEP facilitation when the width of the region with weak CS intensity was between 10 and 15 mm (Fig. 5B). For Subject 9, however, this deviation from the behavior of the right-handed participants is only due to one data point. On the other hand, in Experiment 2, Subject 3 is the one that exhibited weak SICI at all applied CS intensities at the 2.5-ms ISI (Fig. 4B).

Given that Hannah et al. (2017), who compared conditioning stimuli with 30- and 120-μs periods of rising current, reported that SICI for PA-oriented stimuli increased with CS pulse duration, our variable CS waveform might have slightly affected our results in those experiments in which the pulse duration was varied (in Experiment 3, the CS waveform was fixed). However, it is not straightforward to translate their findings to our study due to differences between the stimulation waveforms used in these studies (e.g., in Experiments 1a, 1b, and 2, the duration of the rising phase of the conditioning stimuli was 10.1–44.4 μs, and our waveforms contained a 30-μs hold period (Koponen et al., 2018b)) and the preliminary nature of their report. On the other hand, variation in our test stimuli was minor (duration of the rising phase was 81.2–86.3 μs) and thus unlikely affected our findings; D'Ostilio et al. (2016) have further reported, e.g., that MEP latency for PA-oriented stimulation is independent of the pulse duration.

We foresee that the demonstrated mTMS technology opens totally new possibilities to study the brain. Future multi-coil transducers (e.g., ones similar to our 5-coil design (Koponen et al., 2018a)) should make it convenient to study functional connections between nearby brain regions, e.g., the supplementary motor area, the primary somatosensory cortex, and M1. Automatic mapping of motor representation areas (Supplementary Fig. S1) or other cortical parameters could also improve clinical practice.

5. Conclusions

Our experiments provided new evidence supporting the view that the inhibition at ISIs of 0.5 and 2.5 ms are of different origin. At both ISIs, APB MEP amplitudes were affected when a conditioning stimulus activated neuronal structures situated within approximately 8 mm from the APB hotspot targeted by a 120%-RMT test stimulus providing an estimate of the size of the cortical region within which SICI (or SICF) originate. In a paired-pulse TMS study in which nearby targets are stimulated, one should carefully control for the spatial distribution of the E-field, as we found similar SICI for a translated conditioning stimulus and a non-translated conditioning stimulus with matched E-field intensities at the APB hotspot. As we demonstrated, mTMS with electronic control of the stimulus location allows studies in which nearby targets are stimulated at millisecond-scale intervals.

Conflict-of-interest statement

J.O.N. and N.M. have received unrelated consulting fees from Nexstim Plc, and R.J.I. is an advisor and a minority shareholder of the company. J.O.N., L.M.K., and R.J.I. are inventors on patent applications on mTMS technology. The other authors declare no conflict of interest.

Acknowledgements

This research has received funding from the Academy of Finland (Decisions No. 255347, 265680, 294625, and 306845), the Finnish Cultural Foundation, and Erasmus Mundus SMART^2 (No. 552042-EM-1-2014-1-FR-ERA MUNDUSEMA2). The authors acknowledge the computational resources provided by the Aalto Science-IT project. The coil former was manufactured by Enna Rane (Aalto University Design Factory). The power cords of the coils and their connectors were donated by Nexstim Plc. The authors thank Tuomas Mutanen for help in the experiments.

Supplementary data

Supplementary data to this article can be found online at https://doi.org/10.1016/j.neuroimage.2019.116194.

Appendix. Adjustment of stimulation intensity based on pulse waveform

Here we describe how the pulse waveforms were varied to adjust the stimulation intensity. We used this methodology both to change the stimulation target and to stimulate the same target (APB hotspot) at two different intensities at millisecond-scale ISIs.

In principle, the stimulation intensity, which depends on the capacitor voltages, and the E-field profile, which depends on the ratio of the capacitor voltages, in mTMS could be changed by adjusting the capacitor voltages. This kind of adjustment, however, is inherently slow and may take from a few tens of milliseconds to seconds. To overcome this limitation, we adjusted the duration of the initial positive phase of the stimulation waveform to obtain the desired amount of neuronal membrane polarization (Peterchev et al., 2013) in the presence of a given capacitor voltage (Fig. A1).

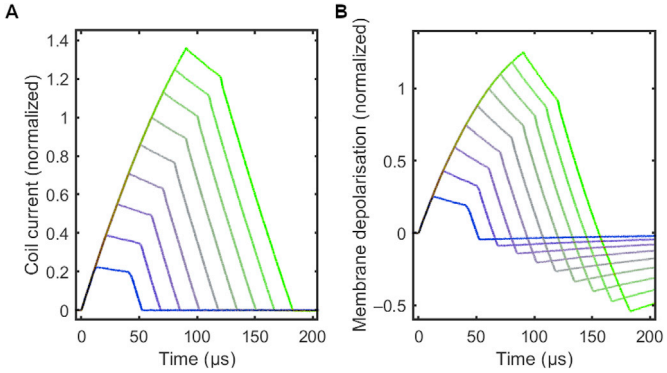

Fig. A.1. Adjusting stimulation intensity by varying the pulse waveform. (**A**) Measured current waveforms at a fixed capacitor voltage for pulses with different durations. (**B**) Calculated membrane depolarization due to the waveforms of (**A**); here, we have assumed a 200-μs neuronal time constant. The data are normalized to those of pulses with a 60-μs initial phase. The colors link the data of the two panels.

We modeled the effect of the pulse waveform on the polarization of the neuronal membrane by assuming a 200-μs cellular time constant (Barker et al., 1991; Peterchev et al., 2013). To make the pulses match each other in terms of non-linear effects of the neuronal membrane (Koponen et al., 2018b), the positive and negative phases of the induced E-field were separated by a 30-μs hold period of near-zero E-field intensity (Fig. A1).

In those paired-pulse mTMS protocols in which the conditioning stimulus was administered to a target within 15 mm from the APB hotspot, the capacitor voltages and pulse durations were set so that the subsequent test stimulus would have the desired strength without any voltage adjustment. In these protocols, the test stimuli were administered using the figure-of-eight coil only. When the transducer was placed between the two targets, the polarity of the current in the oval coil was reversed between the two pulses and the adjustment of the pulse duration was used to compensate for the reduction in capacitor voltages due to the conditioning stimulus.

References

Asanuma, H., Okuda, O., 1962. Effects of transcallosal volleys on pyramidal tract cell activity of cat. J. Neurophysiol. 25, 198–208. https://doi.org/10.1152/jn.1962.25.2.198.

Ashby, P., Reynolds, C., Wennberg, R., Lozano, A.M., Rothwell, J., 1999. On the focal nature of inhibition and facilitation in the human motor cortex. Clin. Neurophysiol. 110, 550–555. https://doi.org/10.1016/S1388-2457(98)00082-0.

Barker, A.T., Garnham, C.W., Freeston, I.L., 1991. Magnetic nerve stimulation: the effect of waveform on efficiency, determination of neural membrane time constants and the measurement of stimulator output. Electroencephalogr. Clin. Neurophysiol. Suppl. 43, 227–237.

Bohning, D.E., He, L., George, M.S., Epstein, C.M., 2001. Deconvolution of transcranial magnetic stimulation (TMS) maps. J. Neural Transm. 108, 35–52. https://doi.org/10.1007/s007020170095.

Di Lazzaro, V., Oliviero, A., Meglio, M., Cioni, B., Tamburrini, G., Tonali, P., Rothwell, J.C., 2000. Direct demonstration of the effect of lorazepam on the excitability of the human motor cortex. Clin. Neurophysiol. 111, 794–799. https://doi.org/10.1016/S1388-2457(99)00314-4.

Di Lazzaro, V., Pilato, F., Dileone, M., Ranieri, F., Ricci, V., Profice, P., Bria, P., Tonali, P.A., Ziemann, U., 2006. $GABA_A$ receptor subtype specific enhancement of inhibition in human motor cortex. J. Physiol. 575, 721–726. https://doi.org/10.1113/jphysiol.2006.114694.

Di Lazzaro, V., Restuccia, D., Oliviero, A., Profice, P., Ferrara, L., Insola, A., Mazzone, P., Tonali, P., Rothwell, J.C., 1998. Magnetic transcranial stimulation at intensities below active motor threshold activates intracortical inhibitory circuits. Exp. Brain Res. 119, 265–268. https://doi.org/10.1007/s002210050341.

D'Ostilio, K., Goetz, S.M., Hannah, R., Ciocca, M., Chieffo, R., Chen, J.-C.A., Peterchev, A.V., Rothwell, J.C., 2016. Effect of coil orientation on strength–duration time constant and I-wave activation with controllable pulse parameter transcranial magnetic stimulation. Clin. Neurophysiol. 127, 675–683. https://doi.org/10.1016/j.clinph.2015.05.017.

Dubbioso, R., Raffin, E., Karabanov, A., Thielscher, A., Siebner, H.R., 2017. Centre-surround organization of fast sensorimotor integration in human motor hand area. Neuroimage 158, 37–47. https://doi.org/10.1016/j.neuroimage.2017.06.063.

Fang, Q., Boas, D.A., 2009. Tetrahedral mesh generation from volumetric binary and grayscale images. In: 2009 IEEE International Symposium on Biomedical Imaging: from Nano to Macro, pp. 1142–1145. https://doi.org/10.1109/ISBI.2009.5193259.

Fischl, B., 2012. FreeSurfer. Neuroimage 62, 774–781. https://doi.org/10.1016/j.neuroimage.2012.01.021.

Fisher, R.J., Nakamura, Y., Bestmann, S., Rothwell, J.C., Bostock, H., 2002. Two phases of intracortical inhibition revealed by transcranial magnetic threshold tracking. Exp. Brain Res. 143, 240–248. https://doi.org/10.1007/s00221-001-0988-2.

Hanajima, R., Furubayashi, T., Kobayashi Iwata, N., Shiio, Y., Okabe, S., Kanazawa, I., Ugawa, Y., 2003. Further evidence to support different mechanisms underlying intracortical inhibition of the motor cortex. Exp. Brain Res. 151, 427–434. https://doi.org/10.1007/s00221-003-1455-z.

Hannah, R., Tremblay, S., Rocchi, L., Rothwell, J.C., 2017. Dependence of short-interval intracortical inhibition on conditioning pulse duration. Brain Stimul. 10, 471–472. https://doi.org/10.1016/j.brs.2017.01.382.

Ilić, T.V., Meintzschel, F., Cleff, U., Ruge, D., Kessler, K.R., Ziemann, U., 2002. Short-interval paired-pulse inhibition and facilitation of human motor cortex: the dimension of stimulus intensity. J. Physiol. 545, 153–167. https://doi.org/10.1113/jphysiol.2002.030122.

Koponen, L.M., Nieminen, J.O., Ilmoniemi, R.J., 2018a. Multi-locus transcranial magnetic stimulation—theory and implementation. Brain Stimul. 11, 849–855. https://doi.org/10.1016/J.BRS.2018.03.014.

Koponen, L.M., Nieminen, J.O., Mutanen, T.P., Ilmoniemi, R.J., 2018b. Noninvasive extraction of microsecond-scale dynamics from human motor cortex. Hum. Brain Mapp. 39, 2405–2411. https://doi.org/10.1002/hbm.24010.

Koponen, L.M., Nieminen, J.O., Mutanen, T.P., Stenroos, M., Ilmoniemi, R.J., 2017. Coil optimisation for transcranial magnetic stimulation in realistic head geometry. Brain Stimul. 10, 795–805. https://doi.org/10.1016/j.brs.2017.04.001.

Kujirai, T., Caramia, M.D., Rothwell, J.C., Day, B.L., Thompson, P.D., Ferbert, A., Wroe, S., Asselman, P., Marsden, C.D., 1993. Corticocortical inhibition in human motor cortex. J. Physiol. 471, 501–519. https://doi.org/10.1113/jphysiol.1993.sp019912.

Maris, E., Oostenveld, R., 2007. Nonparametric statistical testing of EEG- and MEG-data. J. Neurosci. Methods 164, 177–190. https://doi.org/10.1016/j.jneumeth.2007.03.024.

Nakamura, H., Kitagawa, H., Kawaguchi, Y., Tsuji, H., 1997. Intracortical facilitation and inhibition after transcranial magnetic stimulation in conscious humans. J. Physiol. 498, 817–823. https://doi.org/10.1113/jphysiol.1997.sp021905.

Nieminen, J.O., Koponen, L.M., Ilmoniemi, R.J., 2015. Experimental characterization of the electric field distribution induced by TMS devices. Brain Stimul. 8, 582–589. https://doi.org/10.1016/j.brs.2015.01.004.

Peterchev, A.V., Goetz, S.M., Westin, G.G., Luber, B., Lisanby, S.H., 2013. Pulse width dependence of motor threshold and input–output curve characterized with controllable pulse parameter transcranial magnetic stimulation. Clin. Neurophysiol. 124, 1364–1372. https://doi.org/10.1016/j.clinph.2013.01.011.

Peurala, S.H., Müller-Dahlhaus, J.F.M., Arai, N., Ziemann, U., 2008. Interference of short-interval intracortical inhibition (SICI) and short-interval intracortical facilitation (SICF). Clin. Neurophysiol. 119, 2291–2297. https://doi.org/10.1016/j.clinph.2008.05.031.

Pitkänen, M., Kallioniemi, E., Julkunen, P., Nazarova, M., Nieminen, J.O., Ilmoniemi, R.J., 2017. Minimum-norm estimation of motor representations in navigated TMS mappings. Brain Topogr. 30, 711–722. https://doi.org/10.1007/s10548-017-0577-8.

Raffin, E., Pellegrino, G., Di Lazzaro, V., Thielscher, A., Siebner, H.R., 2015. Bringing transcranial mapping into shape: sulcus-aligned mapping captures motor somatotopy in human primary motor hand area. Neuroimage 120, 164–175. https://doi.org/10.1016/j.neuroimage.2015.07.024.

Raffin, E., Siebner, H.R., 2019. Use-dependent plasticity in human primary motor hand area: synergistic interplay between training and immobilization. Cerebr. Cortex 29, 356–371. https://doi.org/10.1093/cercor/bhy226.

Roshan, L., Paradiso, G.O., Chen, R., 2003. Two phases of short-interval intracortical inhibition. Exp. Brain Res. 151, 330–337. https://doi.org/10.1007/s00221-003-1502-9.

Rothwell, J.C., Hallett, M., Berardelli, A., Eisen, A., Rossini, P., Paulus, W., 1999. Magnetic stimulation: motor evoked potentials. Electroencephalogr. Clin. Neurophysiol. Suppl. 52, 97–103.

Salo, K.S.-T., Vaalto, S.M.I., Koponen, L.M., Nieminen, J.O., Ilmoniemi, R.J., 2019. The effect of experimental pain on short-interval intracortical inhibition with multi-locus transcranial magnetic stimulation. Exp. Brain Res. 237, 1503–1510. https://doi.org/10.1007/s00221-019-05502-5.

Schäfer, M., Biesecker, J.C., Schulze-Bonhage, A., Ferbert, A., 1997. Transcranial magnetic double stimulation: influence of the intensity of the conditioning stimulus. Electroencephalogr. Clin. Neurophysiol./ Electromyogr. Mot. Control 105, 462–469. https://doi.org/10.1016/S0924-980X(97)00054-4.

Stenroos, M., Koponen, L.M., 2019. Real-time computation of the TMS-induced electric field in a realistic head model. Neuroimage (in press). https://doi.org/10.1016/j.neuroimage.2019.116159.

Thickbroom, G.W., Sammut, R., Mastaglia, F.L., 1998. Magnetic stimulation mapping of motor cortex: factors contributing to map area. Electroencephalogr. Clin. Neurophysiol./ Electromyogr. Mot. Control 109, 79–84. https://doi.org/10.1016/S0924-980X(98)00006-X.

Thielscher, A., Kammer, T., 2002. Linking physics with physiology in TMS: a sphere field model to determine the cortical stimulation site in TMS. Neuroimage 17, 1117–1130. https://doi.org/10.1006/nimg.2002.1282.

Vaalto, S., Säisänen, L., Könönen, M., Julkunen, P., Hukkanen, T., Määttä, S., Karhu, J., 2011. Corticospinal output and cortical excitation-inhibition balance in distal hand muscle representations in nonprimary motor area. Hum. Brain Mapp. 32, 1692–1703. https://doi.org/10.1002/hbm.21137.

Vucic, S., Cheah, B.C., Kiernan, M.C., 2011. Dissecting the nechanisms underlying short-interval intracortical inhibition using exercise. Cerebr. Cortex 21, 1639–1644. https://doi.org/10.1093/cercor/bhq235.

Vucic, S., Cheah, B.C., Krishnan, A.V., Burke, D., Kiernan, M.C., 2009. The effects of alterations in conditioning stimulus intensity on short interval intracortical inhibition. Brain Res. 1273, 39–47. https://doi.org/10.1016/j.brainres.2009.03.043.

Vucic, S., Howells, J., Trevillion, L., Kiernan, M.C., 2006. Assessment of cortical excitability using threshold tracking techniques. Muscle Nerve 33, 477–486. https://doi.org/10.1002/mus.20481.

Wassermann, E.M., McShane, L.M., Hallett, M., Cohen, L.G., 1992. Noninvasive mapping of muscle representations in human motor cortex. Electroencephalogr. Clin. Neurophysiology Evoked Potentials Sect. 85, 1–8. https://doi.org/10.1016/0168-5597(92)90094-R.

Windhoff, M., Opitz, A., Thielscher, A., 2013. Electric field calculations in brain stimulation based on finite elements: an optimized processing pipeline for the generation and usage of accurate individual head models. Hum. Brain Mapp. 34, 923–935. https://doi.org/10.1002/hbm.21479.

Ziemann, U., Lönnecker, S., Steinhoff, B.J., Paulus, W., 1996a. Effects of antiepileptic drugs on motor cortex excitability in humans: a transcranial magnetic stimulation study. Ann. Neurol. 40, 367–378. https://doi.org/10.1002/ana.410400306.

Ziemann, U., Rothwell, J.C., Ridding, M.C., 1996b. Interaction between intracortical inhibition and facilitation in human motor cortex. J. Physiol. 496, 873–881. https://doi.org/10.1113/jphysiol.1996.sp021734.